Repository Istituzionale dei Prodotti della Ricerca del Politecnico di Bari

Fast network joining algorithms in industrial IEEE 802.15.4 deployments

This is a pre-print of the following article

Original Citation:
Fast network joining algorithms in industrial IEEE 802.15.4 deployments / Vogli, Elvis; Ribezzo, Giuseppe; Grieco, Luigi Alfredo; Boggia, Gennaro. - In: AD HOC NETWORKS. - ISSN 1570-8705. - 69:(2018), pp. 65-75. [10.1016/j.adhoc.2017.10.013]

Availability:
This version is available at http://hdl.handle.net/11589/117856 since: 2022-06-21

Published version
DOI:10.1016/j.adhoc.2017.10.013

Publisher:

Terms of use:

(Article begins on next page)

12 October 2024

Fast network joining algorithms in Industrial IEEE 802.15.4 deployments

Elvis Vogli, Giuseppe Ribezzo, L. Alfredo Grieco, and Gennaro Boggia
Dep. of Electrical and Information Engineering (DEI)
Politecnico di Bari, v. Orabona 4, 70125, Bari, Italy
e-mail: {name.surname}@poliba.it.

Abstract

Time Slotted Channel Hopping (TSCH) Medium Access Control (MAC) is a key feature of the IEEE 802.15.4 standard, aimed at accommodating the requirements of industrial Internet of Things systems. Time Division Multiple Access (TDMA) is a main pillar of TSCH, on top of which frequency hopping is added to increase the resilience of short range radio links. A tight synchronization among the network nodes is required in TSCH. Luckily, once a node joins the network, several lean techniques can be used to keep alive its synchronization. On contrary, the subtleties of the joining phase in TSCH still deserve investigations since they could hinder an effective usage of the TSCH MAC. To this end, the problem of acquiring the first synchronization in a TSCH network is investigated hereby, from several perspectives: (i) four novel mechanisms are proposed and implemented in real motes to speed up joining operations; (ii) their average joining time is analytically modeled with closed form expressions as a function of node density, communication reliability, and beacon transmission frequency; (iii) their effectiveness and the agreement between experimental and theoretical outcomes are evaluated in several scenarios.

Keywords: Synchronization, IEEE 802.15.4, Time Slotted Channel Hopping, Industrial Internet of Things.

1. Introduction

Nowadays the Internet of Things (IoT) is at the ground floor of many novel

applications and services, based on capillary interactions among smart objects [1]-[6]. Its adoption in industrial environments sets new requirements to satisfy, which does not usually emerge in plain IoT scenarios, such as: (i) wirelike reliability; (ii) ultra low power (years of battery lifetime or energy harvesting capabilities); and (iii) hard constraints on data latency and throughput [7, 8].

Low power and short range wireless communication technologies are key drivers for industrial IoT systems, since they can enable centralized and distributed sensing and actuation operations thanks to their inherent capabilities of creating networks of smart nodes [9]. In this field, the IEEE 802.15.4 MAC is a leading standard [8]. Its scope has been further extended in the 2015 release [10], which, among other features, includes the TSCH[1] to improve reliability and energy efficiency of short range wireless communications in harsh radio conditions.

In 2013, due to the relevance of using this powerful access scheme, the new Internet Engineering Task Force (IETF) "IPv6 over the TSCH mode of IEEE 802.15.4e" (6tisch) working group has been chartered to define new standards for enabling the usage of IEEE 802.15.4 TSCH also in IPv6 Low-power Lossy Networks (LLN).

When TSCH is enabled, a IEEE 802.15.4 LLN is composed by a set of synchronized nodes arranged in a multi-hop topology. Accordingly, all nodes share a common time slotted baseline, organized as a periodic sequence of slotframes. In this way, it is possible to wake up each single node only when strictly necessary, thus minimizing network duty cycle and energy consumption [12, 13]. The effectiveness of this TDMA scheme can be further improved by adopting channel hopping, which can strongly mitigate the impact of noise and interference[2]. To this end, in TSCH each node switches the physical channel at

[1] TSCH has been originally introduced with the IEEE 802.15.4e amendment released in 2012 [11].

[2] As a matter of fact, the effectiveness of TSCH in noisy environments has been already proved in ISA 110.11a and Wireless HART technologies [14], which are industrial protocol stacks of great renown [15].

each consecutive timeslot by following a pre-assigned sequence, referred to as logical channel. The resulting overall reliability is improved because any error occurring in a given timeslot, due to noise and interference on the used physical channel, can be recovered at the next slot by using a different channel (unless there is a wideband interference). Moreover, since 16 logical channels are defined, it is also possible to enable simultaneous transmissions by neighboring nodes (provided they use different logical channels) and spatial frequency reuse, without incurring collisions [12, 16].

In order to capitalize the advantages brought by TSCH, it is necessary to ensure that the network quickly converges towards a global synchronization point, where all nodes share the same time-slotted baseline. According to the standard, the initial synchronization can be reached by configuring at least one node as synchronizer, usually the Personal Area Network (PAN) coordinator, which is in charge to broadcast Enhanced Beacon (EB) frames. Each EB advertises the Absolute Slot Number (ASN), which is the information on the total number of slots elapsed from the boot up. In this way, as soon as a new joining node receives an EB, it can synch up to the slot-frame structure of the network. After, *it can also start to send EBs on its own in order to broaden the diameter of the network.*

It is worth to note that EBs can be transmitted using TSCH to increase the communication resilience in noisy environments. At the same time, this choice can inflate the time spent by a new node to join the network. In fact, the joining node and the synchronizer one are usually not aligned on the same transmission/reception frequencies (i.e., some extra time could be required in order to allow their switching sequences to intersect at the same channel). In other words, while the synchronizers is sending an EB on a given physical channel, the joining node might be listening another frequency, so that both nodes are forced to remain awake for a long time, till the synchronization is gained, thus worsening also energy efficiency. Furthermore, the transmission of EB from multiple nodes can incurs in collisions.

These problems can be faced using a proper scheduling strategy that drives

the transmission of EBs in order to avoid collisions and quicken as much as possible the joining phase. Unfortunately, the most of contributions proposed so far for the basic version of the IEEE 802.15.4 standard do not immediately apply to the TSCH [17] - [33]. Note that in [34] a similar problem has been discussed with reference to the Time Synchronized Mesh Protocol, i.e., an ancestor of TSCH; as a possible solution, it was proposed to increase the number of nodes involved in sending beacons to reduce the time needed for the join phase of a new node.

Recently, several novel contributions have been also formulated for TSCH [35]-[37]. In [35] it is proposed to increase the slots available for EB transmissions in order to improve the chance to match the channel the joining node is listening to. A completely different approach is pursued in [37], proposing a model to calculate the near-optimal schedule for EB transmissions. In the latter case, the schedule needs to be calculated *a-priori* and made known to every joining node before the network bootstrap. Finally, in [36] lean distributed coordination schemes have been proposed to enable the transmission of EBs from multiple network nodes.

The present contribution extends the findings in [36] in several direction: (i) four novel mechanisms to speed up joining operations are proposed and implemented[3] within the OpenWSN stack [38]; (ii) their performance has been analytically modeled with closed form expressions as a function of node density, communication reliability, and beacon transmission frequency; (iii) their effectiveness and the agreement between analytical and experimental results have been successfully evaluated in different scenarios.

Both theoretical and experimental results demonstrate that: (i) the joining process can be made quicker and quicker by increasing the node density, which contributes an higher aggregate transmission rate of EBs; (ii) a significant speed up can be achieved by coordinating, on a distributed basis, the transmission of EBs sent by network nodes; (iii) a further performance improvement can be pur-

[3]The code will be available as open source software.

sued by allowing a higher beacon transmission frequency by nodes powered by the mains (i.e., without any energy constraints) with respect to nodes supplied by batteries.

The rest of the paper is organized as follows. In Sec. 2, an overview on the IEEE 802.15.4 standard is provided with a major emphasis on TSCH and synchronization mechanisms. In Sec. 3 and Sec. 4, the new synchronization algorithms are illustrated and analytically modeled, respectively. Sec. 5 describes the testbed, reports experimental outcomes, and validates theoretical findings. Finally, Sec. 6 closes the paper and draws future research.

2. An Overview on the IEEE 802.15.4 Time Slotted Channel Hopping

TSCH is now part of the latest version of the IEEE 802.15.4 standard and represents a key feature of the IEEE 802.15.4e amendment [11], conceived to improve the reliability of wireless links and reduce energy consumption in industrial environments [8],[25],[39]-[41].

2.1. Time Slotted Channel Hopping

In the IEEE802.15.4 TSCH, channel hopping is added to time slotted access in order to pursue frequency diversity and, hence, mitigate the effects of interference and multipath fading, which can remarkably degrade the Quality of Service (QoS) of LR-WPANs [25],[39]-[41]. Further advantages brought by channel hopping consist in the possibility to: (i) use frequency diversity schemes to enable simultaneous transmissions on different channels; (ii) minimize the duty cycle thanks to optimal scheduling strategies in the time-frequency domain [42],[43].

With TSCH, the time is organized as a periodic sequence of slot frames, made by several timeslots. Each elementary communication resource is identified by a pair, (t_s, ch_{of}), defining the timeslot, t_s, and the logical channel, ch_{of}, to be used for the transmission of a single MAC frame. Logical channels are translated into physical channels as follows:

$$f = F\{(ASN + ch_{of}) \bmod C\} \tag{1}$$

where f is the physical channel, ASN is the Absolute Slot Number, i.e., the total number of timeslots elapsed since the network deployment; the function $F\{\cdot\}$, realized with a look-up-table, contains the set of available channels; and the value C is the number of available physical frequencies (i.e., it is also the size of the considered look-up-table).

The ASN is incremented at each timeslot and shared by all devices in the network. In particular, $ASN = (k \cdot S + t_s)$, where k defines the slotframe cycle (see Fig. 1) and S is the slotframe size. Moreover, the following constraints hold: $0 \leq t_s \leq S - 1$, and $0 \leq ch_{of} \leq C - 1$.

In an IEEE802.15.4e network, 16 channels are available and a blacklist can be used to restrict the set of allowed channels for coexistence purposes. Note that, if S and C, are relatively prime, the translation function in Eq. (1) assures that each link rotates through k available channels over k slotframe cycles; that is, successive frames on a same link are sent over different physical frequencies in successive k slotframe cycles.

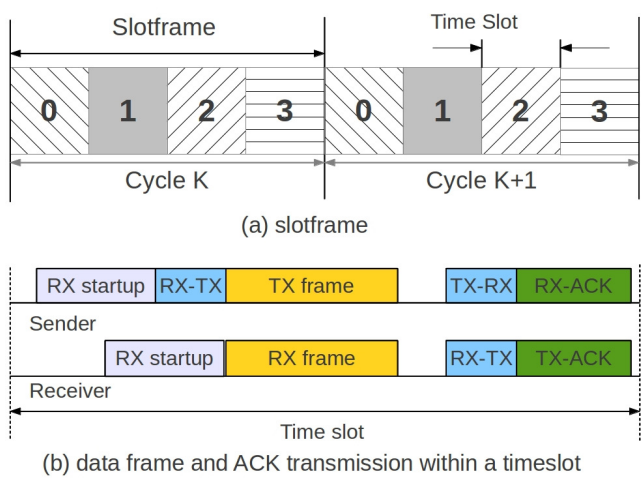

Figure 1: Example of a 4-slot slotframe/timeslot diagram with an acknowledged transmission.

2.2. Synchronization and Network Formation

As shown in Fig. 1, in TSCH a single timeslot is long enough to accomodate the transmission of a maximum length packet, and the reception of its acknowledgement. The duration of a timeslot is implementation-specific: a possible suggested value is 10 ms [11].

The initial network formation is made of two stages: *advertising* and *joining*.

When a TSCH PAN is formed, the PAN coordinator begins to send EBs to advertise the presence of the network.

Any device that wishes to join the network has to wait for the reception of an EB. This listening operation can be executed either "passively" (i.e., using a preferred channel) or "actively" (i.e., scanning different frequencies). After it receives the EB, the new node sends a *Join Request* command frame to the advertising device to actually enter the network. A Join Request, depending on the context, can be processed either locally or by a centralized network manager. Once the request is accepted, the advertiser activates the new node by allocating slot frames and links, which will be used by the newcomer to exchange data with its neighbors. This allocation can be modified over the time to face unexpected changes in the traffic profile and topology (see also [44]).

To broaden the diameter of the network, once synchronized, all Full-Function Devices (FFDs)[4] may send EBs. The advertising rate is configured by a higher layer protocol based on the density of nodes, the desired speed of network formation, and the available energy resources.

It is worth to note that in TSCH, to ensure connectivity among network nodes, synchronization has to be kept alive after joining operations are accomplished. To this end, *Acknowledgement-Based* and *Frame-Based* schemes are defined in the standard, which allow any receiver to calculate the difference be-

[4]Two different device types can participate in an IEEE 802.15.4 network: a full-function device (FFD) and a reduced-function device (RFD). An FFD is a device that is capable of serving as a personal area network (PAN) coordinator or a coordinator. An RFD is a device that is not capable of serving as either a PAN coordinator or a coordinator [10].

tween expected and actual (ACK or frame) arrival times and to tune its clock accordingly to stay synchronized with the sender. Moreover, to maintain synchronization in networks with a very low duty-cycle, keep alive packets are also defined [45].

3. Algorithms for Fast Synchronization

Herein, four novel algorithms to speed up the joining phase in a IEEE 802.15.4e network are developed and described. In what follows, they will be referred to as: Random Vertical filling (RV), Enhanced Coordinated Vertical filling (ECV), Random Horizontal filling (RH), and Enhanced Coordinated Horizontal filling (ECH). Both RV and RH schemes are very lightweight and are meant to moderately boost up joining operations. Instead, ECV and ECH algorithms, (relying on a distributed coordination among nodes) are designed to further improve the performance of RV and RH, at the expense of a slight increase of protocol complexity and of energy spent by coordinator nodes.

In all of them, once a node joins the network it can send its own EBs to speed up joining operations of other joining nodes and increase the network diameter.

The scheduling of EBs is repeated periodically every *multi-slotframe*, which, in turn, is composed by an integer number of slotframes.

It is worth to note that in a given network one and only one of the proposed algorithms can be adopted. It should be advertised in the EBs during network formation. In particular, if the coordinator has no power constraints (i.e., it is powered by the mains) it could adopt one of the enhanced algorithm (i.e., ECV or ECH) in order to provide a better performance in terms of joining time. Otherwise, if energy efficiency requirements prevail on the joining delay, RV or RH algorithms can be used.

Children motes, upon network join, choose the same algorithm as the coordinator to deliver EBs on their own. Instead, during joining operations, a new node only passively listens the channel to catch some EB.

For sake of clarity, Fig. 2 shows an example scheduling structure, which

contains a multi-slotframe lasting five slotframes. A node is allowed to send EBs only in the first timeslot of each slotframe, i.e., the *advertisement* slot. Unless otherwise specified, a node can schedule the transmission of EBs in one and only one advertisement slot of the multi-slotframe. Possible collisions might arise when two or more nodes schedule the transmission of their respective EBs in the same timeslot-channel offset pair.

For each new neighbor that joins the network, the scheduling algorithm shown in Fig. 3 is executed. It runs at each mote in a distributed fashion. A node, after receiving the first EB that enables its synchronization to the network, initializes a schedule for the advertisement of its own EB frames. To avoid collisions, a sensing mechanism can be adopted in ECV and ECH: in this case if candidate slot to EB transmission is sensed busy, then the algorithm recalculates the schedule and repeats the sensing procedure. Otherwise, the EB is transmitted in the candidate slot.

According to the method used to fill the map of the schedule in Fig. 2, the following schemes can be distinguished:

- *Random Vertical filling (RV)* - The coordinator transmits EBs in the first advertisement slot of the multi-slotframe structure using $ch_{of} = 0$. Any newly synchronized node, instead, has to transmit in the same advertisement slot with a randomly chosen channel offset. Thus, each node will fill randomly a cell in the first column of the structure shown in figure 2. However, there is no guarantee that a cell will not be chosen by more than one node. If this happens, *EBs are lost due to collisions*. Fig. 4 shows an example allocation that can be obtained using the Random Vertical filling (RV) algorithm.

- *Enhanced Coordinated Vertical filling (ECV)* - In this case, it is assumed that the coordinator has no energy limitations. Therefore it can transmit EBs in every advertisement slot using $ch_{of} = 0$. This will result in the schedule consisting of all red cells in Fig. 2. Any newly joining node, instead, senses in the advertisement slot of the multi-slotframe structure

all the remaining channels starting from $ch_{of} = 1$ and it schedules the EBs on the first free channel offset. In this way, the first column is progressively filled in the structure shown in the Fig. 2. If the first column results to be completely busy then the node will start sensing the second slotframe starting again from $ch_{of} = 1$. It might happen that two or more nodes choose the same channel offset in the same slotframe, thus generating collisions. To solve this issue (which is quite unlucky to happen) a backoff algorithm could be adopted. Fig. 5 shows an example allocation that can be obtained using the Enhanced Coordinated Vertical filling (ECV) algorithm.

- *Random Horizontal filling (RH)* - The coordinator transmits EBs in the first advertisement slot of the multi-slotframe structure using a $ch_{of} = 0$, whereas a new synchronized node will chose randomly one of the available advertisement slots of the multi-slotframe structure using again a $ch_{of} = 0$. In this way, the first row of advertisement slots in the multi-slotframe structure shown in Fig. 2 is randomly filled. However, there is no guarantee that two or more nodes will not transmit in the same timeslot. If this happens, the EBs will be lost due to collisions. Fig. 6 shows an example allocation that can be obtained using the Random Horizontal filling (RH) algorithm.

- *Enhanced Coordinated Horizontal filling (ECH)* - In this case, it is assumed that the coordinator has no energy limitations therefore it can transmit EBs in every advertisement slot using $ch_{of} = 0$. As a result, referring to the Fig. 2, the first row of advertisement slots is filled by the coordinator. A newly joining node, instead, will start to listen for a free advertisement slot in $ch_{of} = 1$. It will schedule the EB transmission in the first free advertisement slot. If it senses busy all the advertisement slots with $ch_{of} = 1$, the channel offset is incremented and the procedure is repeated until a free slot is found. Also in this case, it might happen that two or ore nodes choose the same slot-channel offset pair. This problem occurs

with a very negligible probability and can be solved using a backoff algorithm. Fig. 7 shows an example allocation that can be obtained using the Enhanced Coordinated Horizontal filling (ECH) algorithm.

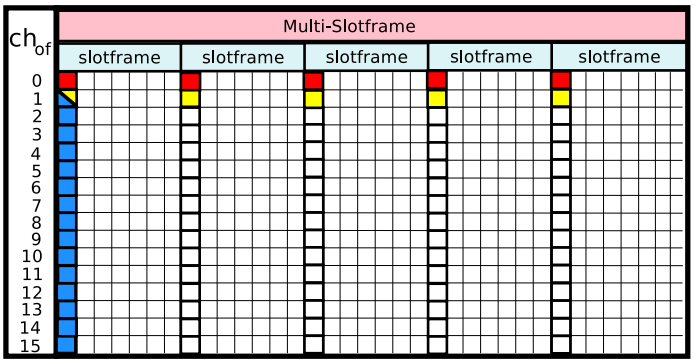

Figure 2: Multi-slotframe structure. In red are shown the slots used by the coordinator for the transmission of EBs, in blue the channel-offset available for vertical algoritms, in yellow the slots used by horizontal algorithms.

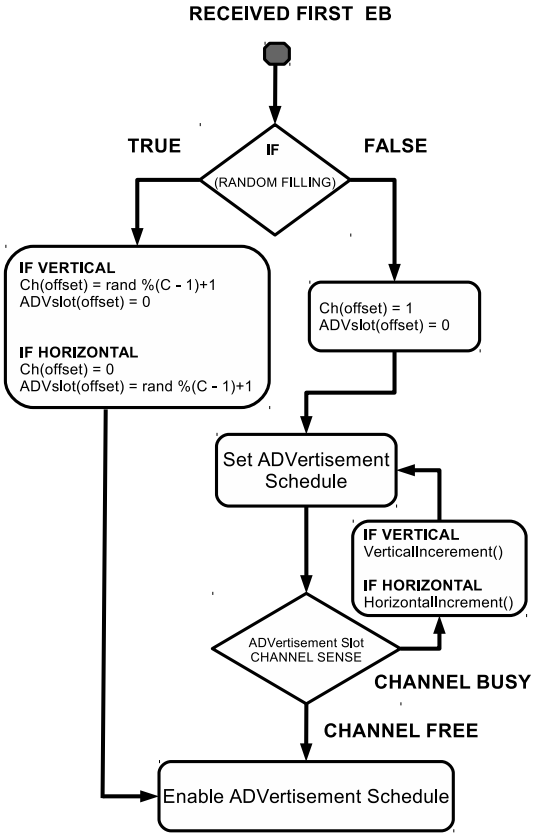

Figure 3: Joining Algorithm.

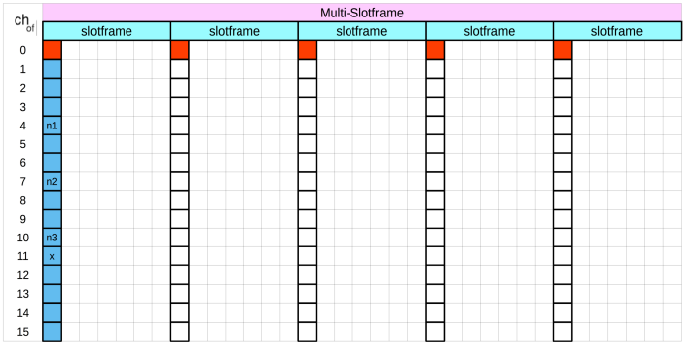

Figure 4: Multi-slotframe structure used by Random Vertical Algorithm. In red are shown the slots used by the coordinator for the transmission of EBs, in blue the channel-offset available for RV algorithm. n1, n2 and n3 are network nodes. It is possible to note a collision on channel 11, due to overlapping slot choice.

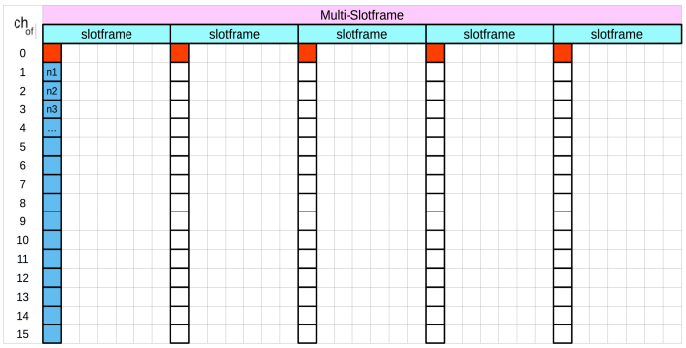

Figure 5: Multi-slotframe structure used by Enhanced Coordinated Vertical Algorithm. In this case, the channel are filled in sequentially. It is possible noting that collision cannot happen anymore.

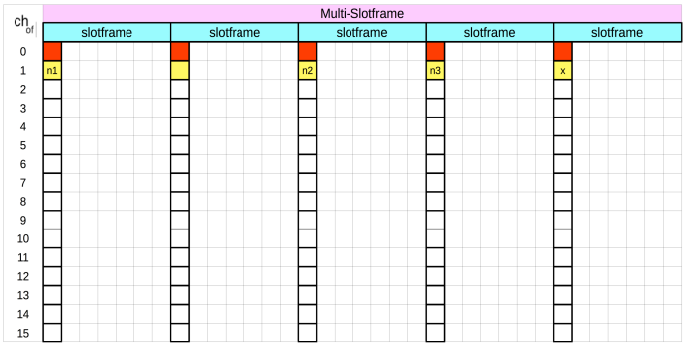

Figure 6: Multi-slotframe structure used by Random Horizontal Algorithm. In red are shown the slots used by the coordinator for the transmission of EBs, in yellow the slots used by RH algorithm. In this case n1, n2 and n3 are network nodes and a collision on slotframe 4.

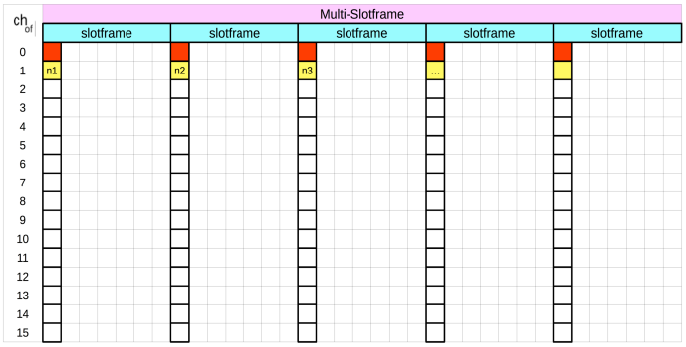

Figure 7: Multi-slotframe structure used by Enhanced Coordinated Horizontal Algorithm. Also in this case, the multi-slotframe structure is filled sequentially and collision are avoided.

4. Analytical Models

As previously discussed in Sec. 2, a node willing to join the network needs to receive an EB. Unfortunately, when using TSCH, the frequency used for transmitting the EB changes during time according to the Eq. (1). As a consequence, the time required to complete the join procedure depends on the probability that the joining node is listening on the same frequency channel where the EB is being transmitted. In the previous section, four algorithms have been designed to speed up joining operations.

Herein, they are analytically modeled to derive the average joining time of a new node A entering in the network.

All the analytical models are based on the following assumptions (unless otherwise specified):

- there are N nodes, already synchronized, in radio visibility that send EBs. They will be referred to as "synchronizer" nodes.
- The EBs are sent by each synchronizer node with a frequency $1/T_M$ where T_M is the multi-slotframe duration.
- Given a timeslot, the probability that a synchronizer node transmits at a certain frequency is uniformly distributed and it is equal to $1/C$, where C is the number of channels in use. This assumption is straightforward to proof since the total number of channels is C and there is no reason a synchronizer node chooses one of them more likely than others.
- The joining node is tuned on one and only one of the available channels, namely f_A, listening for an EB. This is a valid assumption under the condition that the "listening" node switches between frequencies very slowly with respect to the TSCH of the synchronizer.
- The nodes willing to join the network have initially a duty-cycle equal to 100 %, that is, their radios are always on, till they gain the synchronization.

Several possible scenarios are considered in the sequel, taking into account the most typical conditions a new node A has to face when one of the four algorithms defined in Sec. 3 is used. In Table 1, the notation adopted hereafter is summarized.

Table 1: List of used symbols.

Symbol	Definition
A	Joining node
C	Number of channels in TSCH schedule
f_A	Listening channel of the joining node
f_B	Transmission channel of the EB
T_M	Multi-slotframe duration
γ_C	Mean number of channels where only one EB is transmitted
M_T	Average period for EB transmission
M_S	Number of T_M periods needed for synchronization
N	Number of synchronized nodes
N^*	Optimal number of nodes
P_1	Probability that a channel is selected for the beacon transmission by only one node
Π_D	Packet delivery ratio
S_f	Number of slotframes within an EB period
T_f	Slotframe period
T_S	Average synchronization time
T_S^*	Optimal synchronization time
U_f	Mean number of advertisement slots where only one EB is transmitted

4.1. Random Vertical filling model

In the RV scheme, the EB transmission is allowed to each synchronizer node in only one timeslot every slotframe and the corresponding channel is chosen randomly. Under these hypotheses and given that EBs are sent by N different nodes (already synchronized), collisions among beacons might occur, thus impairing synchronization operations.

Accordingly, the joining node A acquires the synchronization if one and only one synchronizer node transmits the EB on the channel f_A.

The probability, P_1, that one and only one EB is transmitted in f_A can be expressed as the probability that only one synchronizer node sends the EB on the channel f_A (this happens with probability $1/C$) while the remaining $N-1$ ones are using different channels, which happens with probability $(1-1/C)^{N-1}$. Accordingly, the resulting P_1 is:

$$P_1 = N \cdot \frac{1}{C} \cdot \left(1 - \frac{1}{C}\right)^{N-1} . \tag{2}$$

As a consequence, the number of channels γ_C (on average) in which one and only one EB is transmitted can be evaluated by multiplying the total number of channels C by P_1:

$$\gamma_C = C \cdot P_1 = N \cdot \left(1 - \frac{1}{C}\right)^{N-1} . \tag{3}$$

To derive the mean synchronization time, a simplified scenario is firstly considered with $N = 1$ and a packet delivery ratio, Π_D, equal to 1, i.e., there are no errors affecting the EB frames. Under these circumstances, the number of T_M periods, M_S, needed to join the network can be modeled as an uniform discrete random variable ranging from 1 to C. In fact, in the best case, the EB is sent on f_A in the first multi-slotframe starting immediately after the joining node begins listening for EBs. On the opposite, in the worst case, the f_A channel will be used after C multi-slotframes. All intermediate cases can occur with the same probability.. Thus, its mean value is given by:

$$\mathbf{E}[M_S] = \frac{C+1}{2} . \tag{4}$$

Now, considering that errors can occur (i.e., $\Pi_D < 1$) and that the mean number of EB transmission retries can be obtained as $1/\Pi_D$, the value $\mathbf{E}[M_S]$ becomes:

$$\mathbf{E}[M_S] = \frac{C+1}{2} \cdot \frac{1}{\Pi_D} \ . \tag{5}$$

The last equation takes into account that, not only the new joining node is tuned on the same channel an EB is being transmitted, but also this transmission is not experiencing errors.

In the more general case with $N > 1$, $\mathbf{E}[M_S]$ is reduced by a factor γ_C because there are (on average) γ_C distinct channels in which one and only one EB is being transmitted. Therefore the following approximation holds:

$$\mathbf{E}[M_S] \cong \frac{C+1}{2} \cdot \frac{1}{\Pi_D} \cdot \frac{1}{\gamma_C} = \frac{C+1}{2N \cdot \Pi_D} \cdot \left(1 - \frac{1}{C}\right)^{1-N} \tag{6}$$

and the average time of synchronization is

$$T_S \cong T_M \cdot \mathbf{E}[M_S] = \frac{T_M\,(C+1)}{2N \cdot \Pi_D} \cdot \left(1 - \frac{1}{C}\right)^{1-N} \ . \tag{7}$$

The optimal number of nodes, N^*, to minimize T_S can be evaluated considering the derivative of T_S with respect to N and setting it to zero:

$$\frac{\partial T_S}{\partial N} = 0 \Rightarrow N^* = -1 \Big/ \ln\left(1 - \frac{1}{C}\right) \ . \tag{8}$$

Substituting N^* in Eq.(7), the optimal synchronization time, T_S^*, is obtained as:

$$T_S^* \cong -\frac{T_M\,(C+1)}{2\Pi_D} \ln\left(1 - \frac{1}{C}\right) e^{[1+\ln(1-1/C)]} \ . \tag{9}$$

4.2. Enhanced Coordinated Vertical filling model

There are two differences with respect to the previous scheme: (i) the PAN coordinator can send beacons in each advertisement slot; (ii) the N nodes that send EBs are coordinated in such a way beacons will rarely collide[5]. The latter condition obviously requires that $N \leq (C-1) \cdot S_f + 1$.

[5]The residual collision probability is accounted in Π_D.

Accordingly, every period T_M, in one preassigned slot, N different EBs will be transmitted, each one on a different channel. In any case, the PAN coordinator sends one EB per slotframe. Therefore, the total number of EBs sent within a T_M period is:

$$B_T = S_f + N - 1 \ . \tag{10}$$

Now, $\mathbf{E}[M_S]$ can be evaluated as in Eq. (6), but considering that in one T_M period many different EBs are transmitted (i.e., a total number of B_T). This increases the opportunity that the joining node is listening on a channel where a given EB is being transmitted; such an event occurs with probability $1/B_T$. Hence,

$$\mathbf{E}[M_S] \cong \frac{C+1}{2\Pi_D} \cdot \frac{1}{B_T} = \frac{C+1}{2\Pi_D} \cdot \frac{1}{S_f + N - 1} \ . \tag{11}$$

The average joining time is:

$$T_S \cong T_M \cdot \mathbf{E}[M_S] = \frac{T_M\,(C+1)}{2\Pi_D\,(S_f + N - 1)} \ . \tag{12}$$

4.3. Random Horizontal filling model

As for the RV model, there are N nodes (including the PAN coordinator) already synchronized that send periodically EB frames with a period equal to $T_M = S_f \cdot T_f$. The novelty in this case is the choice of the timeslot used for the transmission of EBs: each of the N nodes chooses randomly an advertisement slot in the first S_f slotframes (after it joins the network) and it uses always this advertisement slot for transmitting EBs. According to TSCH operations, the physical channel used in the selected slot will be different at every consecutive sloframe.

Thus, we have that a given node selects a specific advertisement slot for EB transmission with a uniform distributed probability equal to $1/S_f$.

Now, following a procedure similar to the one used for obtaining Eq. (2), the probability that a given advertisement slot (and hence a given channel) is chosen by only one of the N nodes within the period T_M is:

$$P_1 = N \cdot \frac{1}{S_f}\left(1 - \frac{1}{S_f}\right)^{N-1} \ . \tag{13}$$

and, consequently, the mean number of successfully used advertisement slots, where there are no collisions among EBs, is:

$$U_f = P_1 \cdot S_f = N \cdot \left(1 - \frac{1}{S_f}\right)^{N-1} . \tag{14}$$

Hence, on an aggregate basis, the average period, M_T, of non collided EB transmissions can be expressed as:

$$M_T \cong \frac{S_f}{U_f} \cdot T_f = \frac{1}{N} \cdot T_M \cdot \left(1 - \frac{1}{S_f}\right)^{1-N} . \tag{15}$$

By following the same approach to derive Eq. (7), it follows that:

$$T_S \cong M_T \cdot \mathbf{E}[M_S] = \frac{M_T\,(C+1)}{2\Pi_D}$$

$$= \frac{T_M\,(C+1)}{2N \cdot \Pi_D} \left(1 - \frac{1}{S_f}\right)^{1-N} . \tag{16}$$

4.4. Enhanced Coordinated Horizontal filling model

With respect to the previous case, there are two novelties: (i) the N nodes (with $N \leq (C-1) \cdot S_f + 1$) sending beacons are coordinated to avoid collisions; (ii) the PAN coordinator sends EBs in every advertisement slot.

Accordingly, the total number of EBs sent within a T_M period is:

$$U_f = S_f + N - 1 . \tag{17}$$

The average period of EB transmission in this case becomes

$$M_T = \frac{T_M}{S_f + N - 1} \tag{18}$$

and the synchronization time is given by

$$T_S \cong M_T \cdot \mathbf{E}[M_S] = \frac{M_T\,(C+1)}{2\Pi_D}$$

$$= \frac{T_M\,(C+1)}{2\Pi_D} \cdot \frac{1}{S_f + N - 1} . \tag{19}$$

4.5. Discussion

In Fig. 8, it is shown the synchronization time as a function of the number of synchronized nodes for all the four algorithms according to the models described above. The time is normalized with respect to the multi-slotframe duration, T_M. In this example, it is assumed that $S_f = C = 16$ and $\Pi_D = 1$. Under these assumptions, it can bee seen the equivalence of RV and RH (ECV and ECH) models. In fact, whereas RH and ECH models spread EB transmissions over different advertisement slots, RV and ECV dilute such transmissions over different channels. Channels and timeslots are equivalent resources from a networking perspective, thus yielding the equivalent behaviors in Fig. 8.

Albeit equivalent for what concerns the average joining time, RV and RH (ECV and ECH, respectively) can accommodate different architectural choices/constraints on the usage of timeslots and channels in real deployments. This motivates their differentiation in this present contribution.

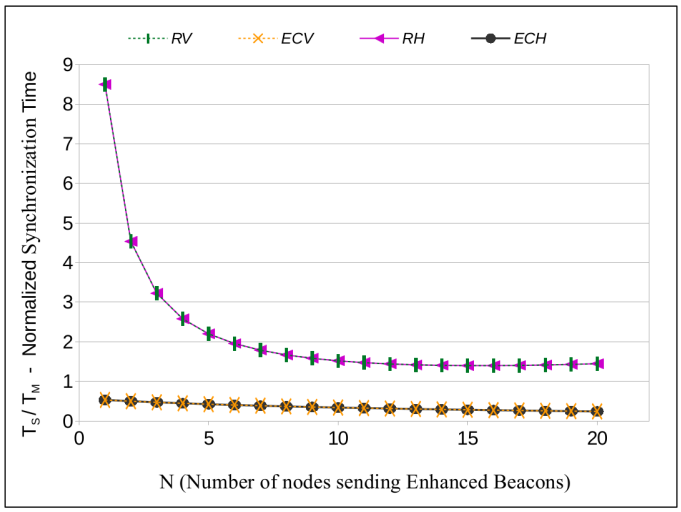

Figure 8: Synchronization time for the models (ideal case: $\Pi_D = 1$).

From the Fig. 8, it can be immediately appreciated the reduction of the joining phase duration in RH and RV for increasing N values. On the other hand, ECH (resp. ECV) greatly improves the network bootstrap with respect

to RH (resp. RV) because EB transmissions are coordinated to avoid collisions and to leverage the capabilities of the PAN coordinator to further speed up the overall joining process by sending more EBs.

5. Experimental evaluation

The algorithms described in this work have been implemented in the *OpenWSN* stack [38]. An extensive experimental campaign was carried out by using TelosB motes. In such experiments, it was used a scheduling structure like the one shown in Fig. 2 with a multi-slotframe of 15 slotframes and each slotframe lasting 101 timeslots.

The topology used for the experiments is pictured in Fig. 9: it is composed by N nodes already synchronized (including the coordinator) that are in radio visibility to each other and with a joining node.

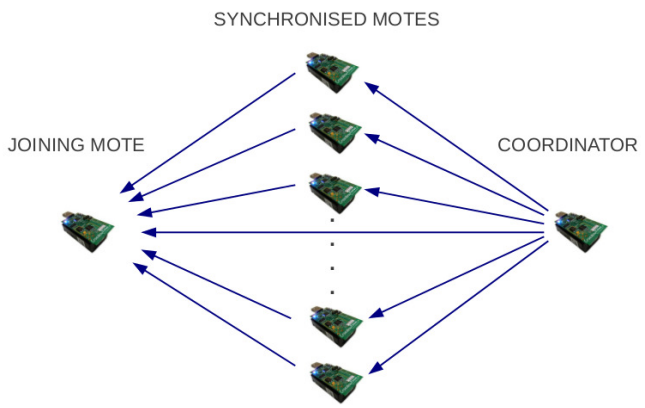

Figure 9: Reference topology used in the experiments.

For each algorithm, the time needed for the joining node to receive the first valid EB was measured.

The *joining node* is configured so that it can provide several measurements of the joining time. In fact, once it successfully receives an EB, it reboots after a random waiting time uniformly distributed in the interval [0, *multi-slotframe*

duration]. After the reboot, it tries to join again the network, thus providing a new measurement of the joining time.

Experiments were held in different scenarios, with N ranging from 1 to 10. In what follows, experimental results are reported, for each algorithm, with a confidence intervals at 95%, evaluated considering 100 samples. In addition, experimental results are compared with respect to the theoretical counterparts derived in sec. 4.

In all the reported graphs the time is normalized to the multi-slotframe duration, T_M.

The experimental results for the RV and RH are shown in Fig. 10 and Fig. 11, respectively. It can be easily recognized the similarity between the model and the experiments. Moreover, by looking at those figures, it is clear that, as N increases, the joining time decreases. This experimentally confirms that the network bootstrap can be effectively sped up by leveraging the capability of already synchronized nodes to send EBs.

Figs. 12 and 13 show that experimental results nicely match analytical models also for the ECV and ECH algorithms.

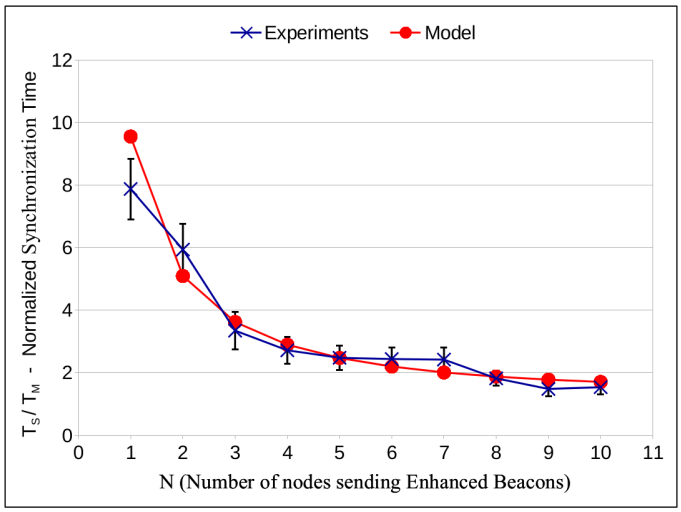

Figure 10: Synchronization time for RV algorithm (Confidence intervals: 95%).

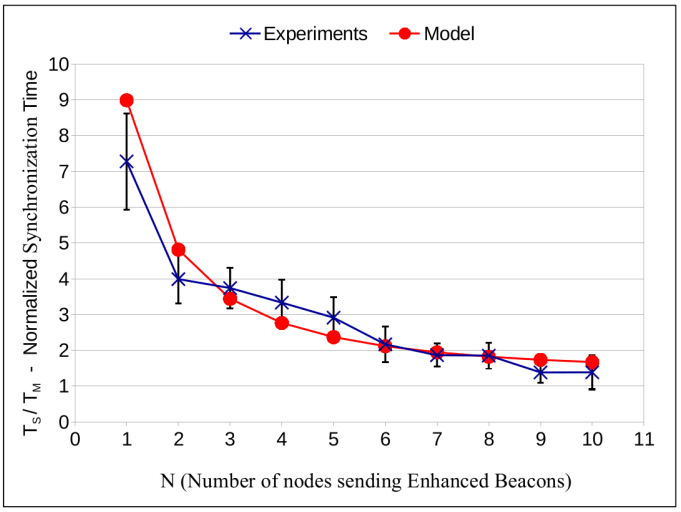

Figure 11: Synchronization time for RH algorithm (Confidence intervals: 95%).

Also, observing the synchronization times, it is worth to note that both ECV and ECH greatly outperform RV and RH thanks to the distributed coordination mechanism they employ, which lowers the collision probability. As a matter of fact, the performance gain is about one order of magnitude for $N = 10$ and two orders of magnitude for $N = 1$.

It is worth to note that the schemes proposed in [37] enhance the performance of RV and RH up to 30%, which is much lower than what can be achieved using ECH and ECV.

To summarize, Table. 2 shows the average error and standard deviation of the synchronization time estimation, obtained by comparing results from analytical models and experimental results. It reports that the average error is below 15% and the standard deviation below 11% for any algorithm. Therefore, from these results, we can conclude that analytical models can be effectively used to correctly estimate the joining time and help designers in adequately sizing real networks.

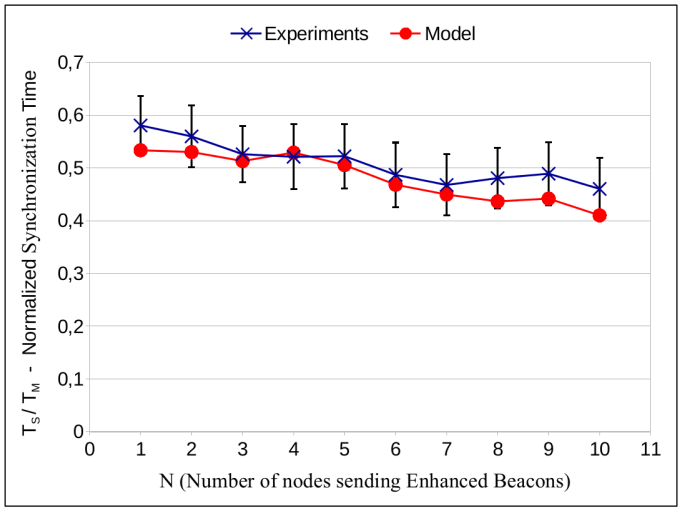

Figure 12: Synchronization time for ECV algorithm (Confidence intervals: 95%).

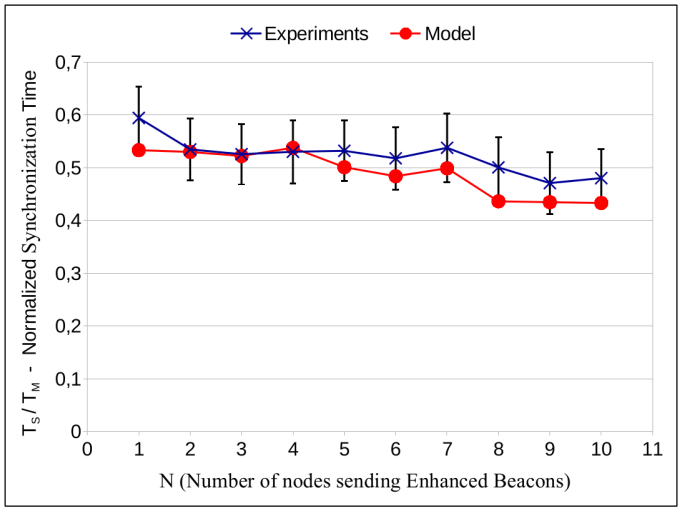

Figure 13: Synchronization time for ECH algorithm (Confidence intervals: 95%).

Table 2: Average model estimation errors and standard deviations.

Algorithm	Average error (%)	standard deviation (%)
RV	10.89	6.41
ECV	10.19	8.45
RH	14.96	10.62
ECH	13.71	9.79

6. Conclusion

This contribution deeply explored the joining phase in a TSCH network from theoretical and experimental points of view. The problems arising from this fundamental stage of a TSCH LLN have been firstly stated and four different algorithms have been proposed to lift the limitations of currently available solutions. Then, the four novel joining schemes have been theoretically modeled in order to derive the average joining time, in close form expressions, as a function of the density of nodes, the transmission frequency of EBs, and the reliability of wireless channels. In addition, the proposed algorithms have been implemented in the OpenWSN platform and tested in realistic scenarios: the tight agreement between theoretical and experimental outcomes confirms both the effectiveness of the proposed joining mechanisms and the usefulness of their model in sizing practical IoT deployments. Finally, it is worth remarking that, to the best of the authors' knowledge, this is the first contribution in literature that proposes lean and straightly deployable distributed algorithms to solve the network bootstrap problem in TSCH networks, together with closed form expressions that can aid network designers in realistic settings. Future research will investigate the effectiveness of proposed algorithms in large scale scenarios.

References

[1] M. K. Lim, W. Bahr, S. C. Leung, RFID in the warehouse: A literature analysis (1995–2010) of its applications, benefits, challenges and future trends, International Journal of Production Economics 145 (1) (2013) 409 – 430.

[2] P. J. Reaidy, A. Gunasekaran, A. Spalanzani, Bottom-up approach based on Internet of Things for order fulfillment in a collaborative warehousing environment, International Journal of Production Economics 159 (2014) 29–40.

[3] L. Zhang, Y. Luo, F. Tao, B. H. Li, L. Ren, X. Zhang, H. Guo, Y. Cheng, A. Hu, Y. Liu, Cloud manufacturing: a new manufacturing paradigm, Enterprise Information Systems 8 (2) (2014) 167–187.

[4] C. Jin, F. Li, M. Wilamowska-Korsak, L. Li, L. Fu, Bsp-ga: A new genetic algorithm for system optimization and excellent schema selection, Systems Research and Behavioral Science 31 (3) (2014) 337–352.

[5] B. Huang, C. Li, F. Tao, A chaos control optimal algorithm for qos-based service composition selection in cloud manufacturing system, Enterprise Information Systems 8 (4) (2014) 445–463.

[6] W. Tan, S. Chen, J. Li, L. Li, T. Wang, X. Hu, A trust evaluation model for e-learning systems, Systems Research and Behavioral Science 31 (3) (2014) 353–365.

[7] L. Grieco, A. Rizzo, S. Colucci, S. Sicari, G. Piro, D. D. Paola, G. Boggia, Iot-aided robotics applications: technological implications, target domains and open issues, Computer Communications 54 (2014) 32 – 47. doi:http://dx.doi.org/10.1016/j.comcom.2014.07.013.

[8] M. Palattella, N. Accettura, X. Vilajosana, T. Watteyne, L. Grieco, G. Boggia, M. Dohler, Standardized Protocol Stack for the Internet of (Important) Things, IEEE Communications Surveys & Tutorials 15 (3) (2013) 1389–1406.

[9] K. Chen, S. Lien, Machine-to-machine communications: Technologies and challenges, Ad Hoc Networks 18 (0) (2014) 3 – 23.

[10] IEEE Standard for Low-Rate Wireless Networks, IEEE Std. 802.15.4, IEEE (April 2016). doi:10.1109/IEEESTD.2016.7460875.

[11] 802.15.4e-2012: IEEE Standard for Local and Metropolitan Area Networks – Part 15.4: Low-Rate Wireless Personal Area Networks (LR-WPANs) Amendment 1: MAC Sublayer (Apr. 2012).

[12] M. R. Palattella, N. Accettura, M. Dohler, L. A. Grieco, G. Boggia, Traffic-Aware Time-Critical Scheduling in Heavily Duty-Cycled IEEE 802.15.4e for an Industrial IoT.

[13] M. Baldi, R. Giacomelli, G. Marchetto, Time-driven access and forwarding for industrial wireless multihop networks, IEEE Transactions on Industrial Informatics 5 (2) (2009) 99–112.

[14] K. Al-Agha, M.-H. Bertin, T. Dang, A. Guitton, P. Minet, T. Val, J.-B. Viollet, Which wireless technology for industrial wireless sensor networks? the development of ocari technology, IEEE Transactions on Industrial Electronics 56 (10) (2009) 4266–4278.

[15] L. Tang, K. Wang, Y. Huang, F. Gu, Channel characterization and link quality assessment of IEEE 802.15.4-compliant radio for factory environments, IEEE Transactions on Industrial Informatics 3 (2) (2007) 99–110.

[16] N. Accettura, M. Palattella, G. Boggia, L. Grieco, M. Dohler, Decentralized traffic aware scheduling for multi-hop low power lossy networks in the Internet of Things, in: IEEE 14th International Symposium and Workshops on a World of Wireless, Mobile and Multimedia Networks,(WoWMoM), 2013, pp. 1–6.

[17] B. Villaverde, R. De Paz Alberola, S. Rea, D. Pesch, Experimental evaluation of beacon scheduling mechanisms for multihop IEEE 802.15.4 wireless sensor networks, in: Fourth International Conference on Sensor Technologies and Applications, (SENSORCOMM), 2010, pp. 226–231.

[18] R. Burda, C. Wietfeld, A distributed and autonomous beacon scheduling algorithm for IEEE 802.15.4/ZigBee networks, in: IEEE Internatonal Conference on Mobile Adhoc and Sensor Systems, (MASS), 2007, pp. 1–6.

[19] H. Jeon, Y. Kim, Bop (beacon-only period) and beacon scheduling for MEU (mesh-enabled usn) devices, in: The 9th International Conference on

Advanced Communication Technology, (ICACT), Vol. 2, 2007, pp. 1139–1142.

[20] E. Kim, H. Choi, Ebbs: Energy-efficient bop-based beacon transmission scheduling for WSNs, in: IEEE 19th International Symposium on Personal, Indoor and Mobile Radio Communications, (PIMRC), 2008, pp. 1–6.

[21] A. Koubaa, A. Cunha, M. Alves, A time division beacon scheduling mechanism for IEEE 802.15.4/Zigbee cluster-tree wireless sensor networks, in: 19th Euromicro Conference on Real-Time Systems,(ECRTS), 2007, pp. 125–135.

[22] Z. Hanzalek, P. Jurčík, Energy efficient scheduling for cluster-tree wireless sensor networks with time-bounded data flows: Application to ieee 802.15.4/zigbee, IEEE Transactions on Industrial Informatics 6 (3) (2010) 438–450.

[23] J. Lu, A. Van Den Bossche, E. Campo, A new beacon scheduling mechanism for mesh wireless personal area networks based on IEEE 802.15.4, in: IEEE 16th Conference on Emerging Technologies Factory Automation, (ETFA), 2011, pp. 1–4.

[24] Y. Huang, A. Pang, H. Hung, A comprehensive analysis of low-power operation for beacon-enabled ieee 802.15.4 wireless networks, IEEE Transactions on Wireless Communications 8 (11) (2009) 5601–5611.

[25] E. Toscano, L. Lo Bello, Multichannel superframe scheduling for ieee 802.15.4 industrial wireless sensor networks, IEEE Transactions on Industrial Informatics 8 (2) (2012) 337–350.

[26] G. Romaniello, E. Potetsianakis, O. Alphand, R. Guizzetti, A. Duda, Fast and energy-efficient topology construction in multi-hop multi-channel 802.15.4 networks, in: IEEE 9th International Conference on Wireless and Mobile Computing, Networking and Communications, (WiMob), 2013, pp. 382–387.

[27] S. Yoo, P. Chong, D. Kim, Y. Doh, M. Pham, E. Choi, J. Huh, Guaranteeing real-time services for industrial wireless sensor networks with ieee 802.15.4, IEEE Transactions on Industrial Electronics 57 (11) (2010) 3868–3876.

[28] N. Torabi, K. Rostamzadeh, V. Leung, IEEE 802.15.4 beaconing strategy and the coexistence problem in ism band, IEEE Transactions on Smart Grid PP (99) (2014) 1–1.

[29] M. Khanafer, M. Guennoun, H. Mouftah, A survey of beacon-enabled IEEE 802.15.4 MAC protocols in wireless sensor networks, IEEE Communications Surveys Tutorials 16 (2) (2014) 856–876.

[30] A. Koubâa, A. Cunha, M. Alves, E. Tovar, Tdbs: a time division beacon scheduling mechanism for zigbee cluster-tree wireless sensor networks, Real-Time Systems 40 (3) (2008) 321–354.

[31] W. Lee, K. Hwang, Y. Jeon, S. Choi, Distributed fast beacon scheduling for mesh networks, in: IEEE 8th International Conference on Mobile Adhoc and Sensor Systems (MASS), 2011, pp. 727–732.

[32] B. Nefzi, D. Khan, Y.-Q. Song, TBoPS: A tree based distributed beacon only period scheduling mechanism for IEEE 802.15.4, in: IEEE 8th International Conference on Distributed Computing in Sensor Systems (DCOSS), 2012, pp. 341–346.

[33] L. Yeh, M. Pan, Beacon scheduling for broadcast and convergecast in zigbee wireless sensor networks, Computer Communications 38 (0) (2014) 1 – 12.

[34] K. S. J. Pister, L. Doherty, TSMP: Time Synchronized Mesh Protocol, in: International Symposium on Distributed Sensor Networks, (DSN), 2008, pp. 391–398.

[35] T. P. Duy, Y. Kim, An efficient joining scheme in IEEE 802.15.4e, in: Information and Communication Technology Convergence (ICTC), 2015 International Conference on, 2015, pp. 226–229.

[36] E. Vogli, G. Ribezzo, L. A. Grieco, G. Boggia, Fast join and synchronization schema in the IEEE 802.15.4e MAC, in: 2015 IEEE Wireless Communications and Networking Conference Workshops, 2015, pp. 85–90.

[37] D. D. Guglielmo, S. Brienza, G. Anastasi, A model-based beacon scheduling algorithm for IEEE 802.15.4e TSCH networks, in: 2016 IEEE 17th International Symposium on A World of Wireless, Mobile and Multimedia Networks (WoWMoM), 2016, pp. 1–9.

[38] T. Watteyne, X. Vilajosana, B. Kerkez, F. Chraim, K. Weekly, Q. Wang, S. D. Glaser, K. S. J. Pister, OpenWSN: a Standards-Based Low-Power Wireless Development Environment, Transactions on Emerging Telecommunications Technologies 23 (5) (2012) 480–493.

[39] L. Lo Bello, E. Toscano, Coexistence issues of multiple co-located IEEE 802.15.4/ZigBee networks running on adjacent radio channels in industrial environments, IEEE Transactions on Industrial Informatics 5 (2) (2009) 157–167.

[40] V. Gungor, B. Lu, G. Hancke, Opportunities and challenges of wireless sensor networks in smart grid, IEEE Transactions on Industrial Electronics 57 (10) (2010) 3557–3564.

[41] G. Anastasi, M. Conti, M. Di Francesco, A comprehensive analysis of the mac unreliability problem in IEEE 802.15.4 wireless sensor networks, IEEE Transactions on Industrial Informatics 7 (1) (2011) 52–65.

[42] T. Watteyne, A. Mehta, K. S. J. Pister, Reliability Through Frequency Diversity: Why Channel Hopping Makes Sense, in: Proceedings of the 6th ACM Symposium on Performance Evaluation of Wireless Ad Hoc, Sensor, and Ubiquitous Networks, (PE-WASUN), 2009, pp. 116–123.

[43] T. Kerkez, B.and Watteyne, M. Magliocco, S. Glaser, K. Pister, Feasibility analysis of controller design for adaptive channel hopping, in: Proceedings

of the Fourth International ICST Conference on Performance Evaluation Methodologies and Tools, (VALUETOOLS), 2009, pp. 76–82.

[44] T. Watteyne, M. Palattella, L. Grieco, Using IEEE 802.15.4e time-slotted channel hopping (TSCH) in the Internet of Things (IoT): Problem statement, RFC 7554, IETF (May 2015).

[45] Stanislowski, D. and Vilajosana, X. and Wang, Q. and Watteyne T. and Pister, K., Adaptive Synchronization in IEEE802.15.4e Networks, IEEE Transactions of Industrial Informatics 10 (1) (2014) 795–802.